ICBatlas: A Comprehensive Resource for Depicting Immune Checkpoint Blockade Therapy Characteristics from Transcriptome Profiles

Mei Yang[1,2], Ya-Ru Miao[1], Gui-Yan Xie[1], Mei Luo[1], Hui Hu[1], Hang Fai Kwok[3,4], Jian Feng[5], and An-Yuan Guo[1,2]

ABSTRACT

Immune checkpoint blockade (ICB) therapy provides remarkable clinical benefits for multiple cancer types. Much work is currently being conducted to investigate the mechanisms of ICB therapy at the transcriptional level. Integrating the data produced by these studies will help us give more insight into the transcriptomic features of ICB therapy. We collected the transcriptome and clinical data of ICB-treated patient samples from the Gene Expression Omnibus, ArrayExpress, The Cancer Genome Atlas, and dbGaP databases. On the basis of the clinical information, all samples are initially classified into response/nonresponse or pretreatment/on-treatment groups. Differential expression, pathway enrichment, and immune cell infiltration analyses are performed between the samples from different groups. We also introduce the Response Score (RS) calculated by integrating the variability degree and the frequency of the dysregulated genes in the responders to evaluate the impact of gene expression on the response. Finally, all the above-mentioned contents are integrated into the ICBatlas database. ICBatlas provides the transcriptome features of ICB therapy through the analysis of 1,515 ICB-treated samples from 25 studies across nine cancer types. The data in ICBatlas include clinical outcomes, treatment-related genes, biological pathways, and immune cell infiltration. Users can investigate the above-mentioned transcriptome features in the response (R vs. NR) or treatment (Pre vs. On) modules at the data set, cancer type, or immune checkpoint level and compare the degree of gene impact on the response in the RS module. ICBatlas is the first database to show the transcriptome features on ICB therapy in human cancers and freely available at http://bioinfo.life.hust.edu.cn/ICBatlas/.

Introduction

Cancer immunotherapy, particularly immune checkpoint blockade (ICB) therapy, has achieved notable clinical success and became the focus of many clinical studies. The primary checkpoint antibodies that target PD-1/PD-L1 or CTLA-4 have demonstrated improved prognosis in patients with skin cutaneous melanoma (SKCM; refs. 1, 2) and patients with other cancer types, such as non–small cell lung cancer (NSCLC), gastric cancer, and bladder cancer (3, 4). Nevertheless, ICB treatment in clinical trials has demonstrated a rather wide range of response rate (10%–40%; refs. 2, 5–7) and approximately 30% relapse (8), which sometimes leads to considerable side effects and costs. Therefore, further studies are needed to determine mechanisms of ICB therapy response and responder characteristics.

With the development of next-generation sequencing, transcriptomics has become a routine technology in biomedical research. The past efforts of characterizing ICB therapy at the transcriptome level focused on the dynamic changes during treatment, the differences between responders and nonresponders (9, 10), resistance mechanisms (11, 12), and immune-related adverse events (13–15). Furthermore, some response-related biomarkers (e.g., cytolytic activity, IFNγ, and GEP) or prediction models (e.g., IMPRES, IPRES, TIDE, and ICGe) derived from transcriptome data were produced (11, 16–20). Unfortunately, most of these signatures showed variable performance in different cohorts. Moreover, with the limited cohort size in each clinical study, it had been challenging to comprehensively determine mechanisms of ICB response. At present, large amounts of ICB-related data are being generated and scattered through public databases [e.g., Gene Expression Omnibus (GEO), ArrayExpress, The Cancer Genome Atlas (TCGA), and the database of Genotypes and Phenotypes (dbGaP)]. Integrating these data will help us gain more insight into the transcriptomic features of the clinical outcome and the mechanisms of ICB therapy.

During the past years, a few ICB therapy-related databases have been developed, including checkpoint therapeutic target database (CKTTD), Tumor Immune Single Cell Hub (TISCH), and Tumor Immune Syngeneic MOuse (TISMO; refs. 21–23). CKTTD (21) compiles immune checkpoint molecules (i.e., proteins, miRNAs, and lncRNAs) and their modulators in cancer immunotherapy curated from literature. TISCH (22) focuses on the immunotherapy-related tumor microenvironment from single-cell data. TISMO (23) was developed to investigate and visualize the transcriptome in syngeneic

[1]Center for Artificial Intelligence Biology, Hubei Bioinformatics and Molecular Imaging Key Laboratory, Key Laboratory of Molecular Biophysics of the Ministry of Education, College of Life Science and Technology, Huazhong University of Science and Technology, Wuhan, China. [2]Research Center of Clinical Medicine, Affiliated Hospital of Nantong University, Nantong, Jiangsu, China. [3]Cancer Centre, Faculty of Health Sciences, University of Macau, Taipa, Macau SAR. [4]MoE Frontiers Science Center for Precision Oncology, University of Macau, Taipa, Macau SAR. [5]Department of Respiratory, Affiliated Hospital of Nantong University, Nantong, Jiangsu, China.

M. Yang, Y.-R. Miao, and G.-Y. Xie contributed equally as the co-senior authors of this article.

Corresponding Authors: An-Yuan Guo, Huazhong University of Science and Technology, 1037 Luoyu Road, Wuhan, 430074, China. E-mail: guoay@hust.edu.cn; and Jian Feng, Affiliated Hospital of Nantong University, NO.20, Xisi Road, Nantong, 226001, China. E-mail: Jfeng68@126.com

Cancer Immunol Res 2022;10:1398–406

doi: 10.1158/2326-6066.CIR-22-0249

mouse models across different ICB treatment and response groups. To date, however, no published database has yet compiled transcriptomic characteristics of ICB therapy based on human data. Consequently, current data resources must be integrated, and a human ICB therapy-related database that can be easily accessed, analyzed, and used by researchers must be presented.

In this study, we construct and draw a large-scale accessible data repository called ICBatlas. ICBatlas is a comprehensive resource depicting the transcriptomic characteristics of ICB therapy based on the gene expression profiles of 1,515 patients from previously published studies across nine cancer types. Overall, ICBatlas provides search, browse, and visualization functions for integrated and reanalyzed results based on large-scale transcriptome data. It is a comprehensive and one-stop solution for transcriptome data-related research on ICB therapy that is freely available at http://bioinfo.life.hust.edu.cn/ICBatlas/.

Materials and Methods

Data collection and metainformation curation

We collected samples of human ICB therapy from GEO, ArrayExpress, TCGA, and dbGaP by searching the keywords "ICB therapy" "immune checkpoint inhibitor therapy" "PD-1/PD-L1" and "CTLA4" (Supplementary Table S1). Both RNA sequencing (RNA-seq) and microarray data were included. We downloaded raw sequencing reads (if available) or other available formats (e.g., raw count, TPM, FPKM, expression matrix of microarray, etc.) for each data set (Supplementary Table S2). Furthermore, the clinical information for the samples, including the cancer type, age, gender, survival time, ICB treatment, and response status, was collected from the original article. The response was based on Response Evaluation Criteria in Solid Tumors v1.1 (24). Responders (R) consisted of patients with complete or partial response and nonresponders (NR) are included patients with either progressive or stable disease. Other six samples with no response outcome were excluded.

Data processing

Different processing methods were applied depending on the data type to obtain more accurate expression values. For the RNA-seq data, raw sequencing reads were downloaded and unpacked through the SRA Toolkit (version 2.9.0-ubuntu64). FastQC (version v0.11.5) was used for data quality control with per base sequence quality >10 and per sequence mean quality scores >27. Trimmomatic (version 0.32) was used for adapter sequence removal and trimming to obtain high-quality clean reads. The clean reads were then mapped to the human reference genome, GRCh38, by HISAT2 (version 2.0.4; ref. 25) and SAMtools (26). StringTie (25) was used to calculate the abundance of transcripts for each sample (i.e., TPM and FPKM). The count data were calculated by FeatureCounts (27). R-package oligo was used to process the raw microarray data. For samples without available raw sequencing reads and microarray data, the expression matrices were downloaded and *log2* transformed: $log2(x + 1)$. ComBat was used to remove the batch effect of samples with batch covariate (28). **Figure 1A** depicts an overview of the data processing workflow.

Differential expression genes and functional enrichment analysis

The differential expression genes (DEG), including protein- and noncoding genes, between R vs. NR and Pre vs. On for the data sets with raw counts of RNA-seq were calculated using DESeq2 (29) with a settled threshold ($|\text{Log}_2$ fold change ($\log_2$FC)$| > 1$ and FDR < 0.05). For samples sequenced by a microarray or those whose raw counts are not available, the Limma (30) package was used to calculate the DEGs with $|\log_2 FC| > 1$ and $P < 0.01$. For each data set, the genes without an expression in more than 70% of the samples were filtered. Gene ontology (GO) and Kyoto Encyclopedia of Genes and Genomes (KEGG) analyses were also performed by using the R-package clusterProfiler (31). The gene set enrichment analysis (GSEA; ref. 32) was used to determine the gene expression signatures that were significantly changed between specific groups. In contrast, the gene set variation analysis (GSVA; ref. 33) was performed to calculate the gene set enrichment score per sample and provide increased power to detect the subtle pathway activity changes between the groups. R-package clusterProfiler and GSVA were implemented with the following gene sets: (i) Cancer hallmark, REACTOME and WikiPathways of Canonical pathways, and C6 (oncogenic signature gene set subset) in Molecular Signature Database version 7.4 (MSigDB, http://www.gsea-msigdb.org/gsea/index.jsp; ii); 17 immune-related pathways from the ImmPort project (ref. 34; https://www.immport.org/); and (iii) MHC and immunomodulatory molecules (35). The statistical significance for the GSVA was evaluated through the Wilcoxon's rank sum test in R language.

Immune analysis by the immune cell abundance identifier

The immune cell abundance identifier (ImmuCellAI; ref. 36) was adopted to estimate the abundance of 24 immune cell types, which are 18 T-cell subsets [i.e., $CD4^+$ T, $CD8^+$ T, naïve $CD4^+$ T, naïve $CD8^+$ T, and cytotoxic T (Tc), exhausted T (Tex), type 1 regulatory T (Tr1), natural regulatory T (nTreg), induced regulatory T (iTreg), T-helpers 1 (Th1), 2 (Th2), and 17 (Th17), follicular T-helper (Tfh), central memory T (Tcm), effector memory T (Tem), natural killer T (NKT), mucosal-associated invariant T (MAIT), and gamma–delta T cells], as well as six other types of immune cells [i.e., B cells, natural killer cells, monocytes, macrophages, neutrophils, and dendritic cells (DC)]. The statistical significance between groups was calculated by the Wilcoxon rank sum test.

Survival analysis

The survival analysis of a specified gene was calculated using a Kaplan–Meier (KM) model through R packages ("survival" and "survminer"). The cox regression analysis was performed to evaluate the impact of genes on prognosis based on the calculated hazard ratio (HR) genes with HR > 1 were defined as risky genes and genes with HR < 1 were defined as protective genes. The *P* values less than 0.05 were considered statistically significant.

Response score calculation

A response score (RS) was introduced to systematically measure the impact power of the DEGs on the ICB response from the data set and cancer type levels. The RS for each gene in the DEGs was calculated as follows:

Data set level:

$$RS = \left(\frac{\sum_{i=1}^{n} log_2 FC}{n} - 1\right) * \sum_{i=1}^{n} T,$$
$$T = \begin{cases} 1, up - regulated\ in\ responders \\ -1,\ down - regulated\ in\ responders \end{cases} \quad (1)$$

where n is the number of data sets with the DEG.

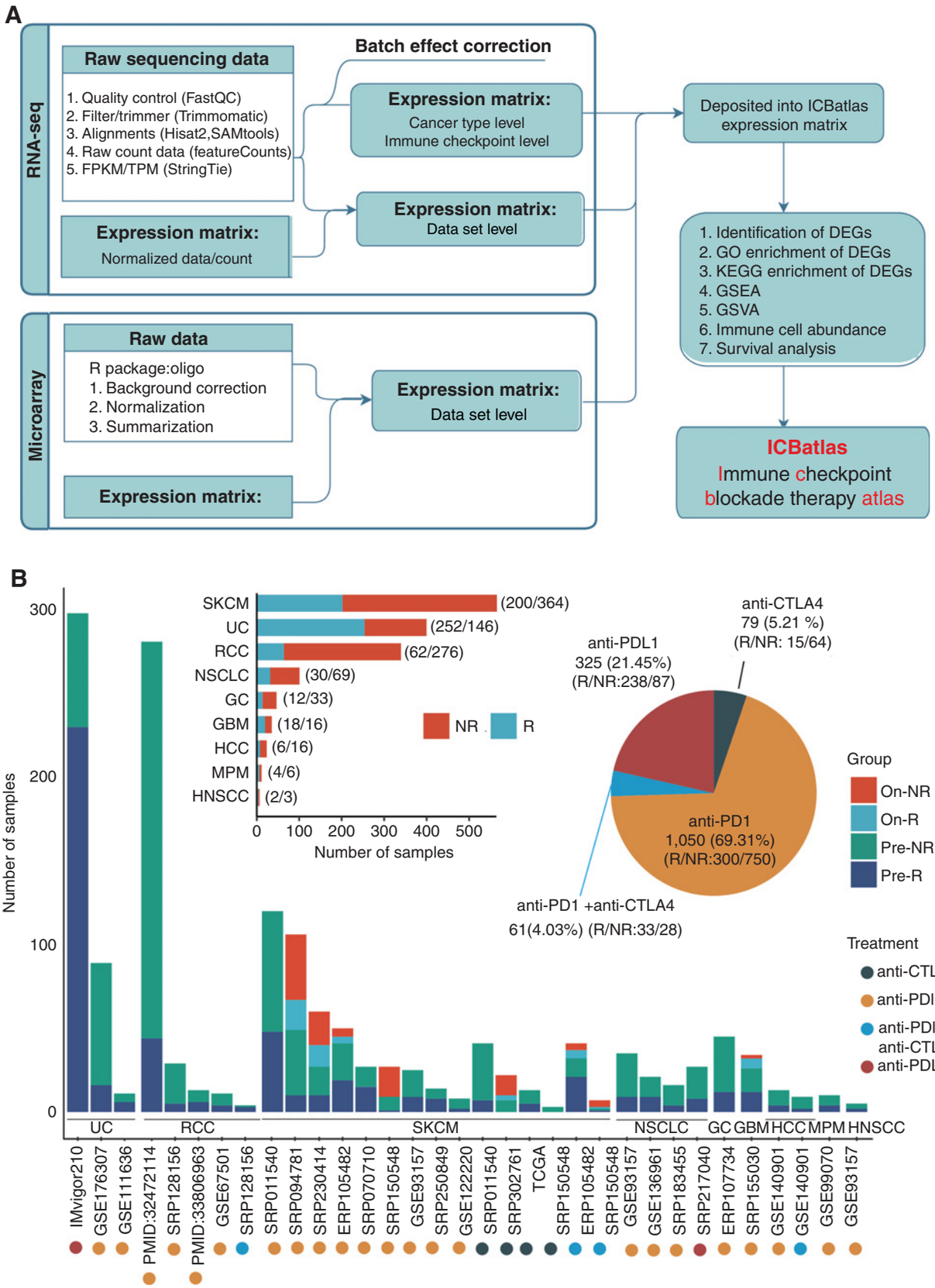

Cancer type level:

$$RS' = \frac{\sum_{i=1}^{m} RS}{m} * \sum_{i=1}^{m} T',$$
$$T' = \begin{cases} 1, & RS \text{ is positive} \\ -1, & RS \text{ is negative} \end{cases}$$

where m is the number of cancer types with specific DEG, and RS is the data set level score of a specific cancer type calculated by Eq. (1). Genes with a positive RS are denoted as positive genes, and their high expression may contribute to a good prognosis of ICB therapy. In contrast, genes with a negative RS are denoted as negative genes, and their high expression may lead to a bad prognosis of ICB therapy. The RS provides researchers with the degree of gene impact on the response from the data set and cancer type levels, which is positively associated with the absolute RS value.

Database development

ICBatlas was run with Python Flask-RESTful API frameworks (https://flask-restful.readthedocs.io/). HTML, CSS, JavaScript (https://angularjs.org), and Bootstrap (https://getbootstrap.com/) were used for the rendering and interactive operations of the front-end pages. The back-end data were organized and queried by MongoDB v3.2 (https://www.mongodb.com/). The charts were manufactured by Echarts and R scripts. The Bootstrap Table was used to construct data tables. Finally, the bioinformatics analyses were implemented by R scripts. ICBatlas is hosted on the Apache HTTP Server (https://httpd.apache.org/).

Data availability

The data analyzed in this study were obtained from published papers are referenced to and publicly available accordingly. The sources of all data sets were shown in Supplementary Table S1.

Results

Data summary of ICBatlas

ICBatlas (http://bioinfo.life.hust.edu.cn/ICBatlas/) encompasses 1515 samples (1,388 RNA-seq and 127 RNA-microarray) treated by PD-1/PD-L1 inhibition, CTLA-4 inhibition, or their combination across nine different cancer types (i.e., SKCM), renal cell carcinoma (RCC), urothelial cancer (UC), hepatocellular carcinoma (HCC), NSCLC, gastric cancer, head and neck squamous cell carcinoma (HNSCC), malignant pleural mesothelioma (MPM), and glioblastoma (GBM) from 25 data sets (**Fig. 1A** and **B**). Among all cancer types, the SKCM samples accounted for the largest proportion (37.18%), followed by UC (26.23%), and other cancer types (**Fig. 1B**). The overall response rate was 38.68% with 586 responders and 929 nonresponders, with a minimum of 18.3% in the RCC and a maximum of 63.3% in the UC. The response rates for the samples in other cancer types (i.e., SCKM, NSCLC, gastric cancer, GBM, HCC, MPM, and HNSCC) ranged from 25% to 40% (**Table 1**, **Fig. 1B**, Supplementary Tables S3 and S4).

Table 1. Summary of meta information of ICBatals database.

	RNA-seq	Microarray	Total
Data sets	19	6	25
Cancer types	6	7	9
Samples	1,388	127	1,515
Pretreatment	1,234	127	1,361
On-treatment	154	—	154
Response	Pre: 494; On: 50	Pre: 42	586
Nonresponse	Pre: 740; On: 104	Pre: 85	929
Cancer			
SKCM	531	33	564
RCC	327	11	338
UC	387	11	398
HCC	—	22	22
NSCLC	64	35	99
GC	45	—	45
HNSCC	—	5	5
MPM	—	10	10
GBM	34	—	34
Target antibody			
Anti–PD-1	932	118	1,050
Anti–PD-L1	325	—	325
Anti-CTLA4	79	—	79
Anti–PD-1+anti-CTLA4	52	9	61

Abbreviations: SKCM, Skin cutaneous melanoma; RCC, renal cell carcinoma; UC, urothelial cancer; HCC, hepatocellular carcinoma; NSCLC, non–small cell lung cancer; GC, gastric cancer; HNSCC, head and neck squamous cell carcinoma; MPM, malignant pleural mesothelioma; GBM, glioblastoma.

Analysis of data in ICBatlas

Data analyses were performed at the data set, cancer type, and immune checkpoint levels. The DEGs, pathway enrichment, immune cell abundance, and survival analysis between responders versus nonresponders (R vs. NR) and pretreatment and on-treatment (Pre vs. On) were performed for each level. The analysis comparing R and NR results indicated that the numbers of significantly enriched hits identified in each data set between R and NR were diverse, demonstrating the data set heterogeneity (**Fig. 2A**–**D**).We observed some shared upregulated genes in responders across different data sets. CXCL10 was significantly upregulated in responders in four melanoma data sets with different treatments, and CXCL9, BAAT, FCGR2C, and P2RY8 were significantly upregulated in responders in three melanoma data sets (**Fig. 2B**). In addition, some signaling pathways were significantly upregulated in the response group in multiple data sets or cancer types, including the negative regulation of the immune system process, cytokine–cytokine receptor interaction, toll-like receptor signaling pathway, and BCR signaling pathway, among others (**Fig. 2C**). The composition and the abundance of immune cells in the tumor microenvironment were also significantly associated with immunotherapy efficacy (36, 37). Hence, in this work, we systematically analyzed the association of immune cell infiltration with ICB therapy by ImmuCellAI, which can calculate the abundance of 24

Figure 1.
Overview of the data statistics and processing in this project. **A,** Overview of the data-processing workflow of ICBatlas. Three types of expression matrices (data set, cancer type, and immune checkpoint levels) were obtained from the raw RNA-seq data. The matrices of cancer type and immune checkpoint level were integrated by different cancer and immune checkpoint with batch effect correction. **B,** Bar plot (large) showing the number of patients collected in each data set. On-R, On-NR, Pre-R, and Pre-NR represent on-treatment response, on-treatment nonresponse, pretreatment response and pretreatment nonresponse, respectively. Treatment (different colors of circular represent differential target antibody). Bar plot (small) showing the number of patients for each cancer type. The numbers in brackets represent the number of patients in the response (R) and nonresponse (NR) groups. Pie chart showing the different target antibody classification. The numbers in brackets represent the number of patients in the response and nonresponse groups.

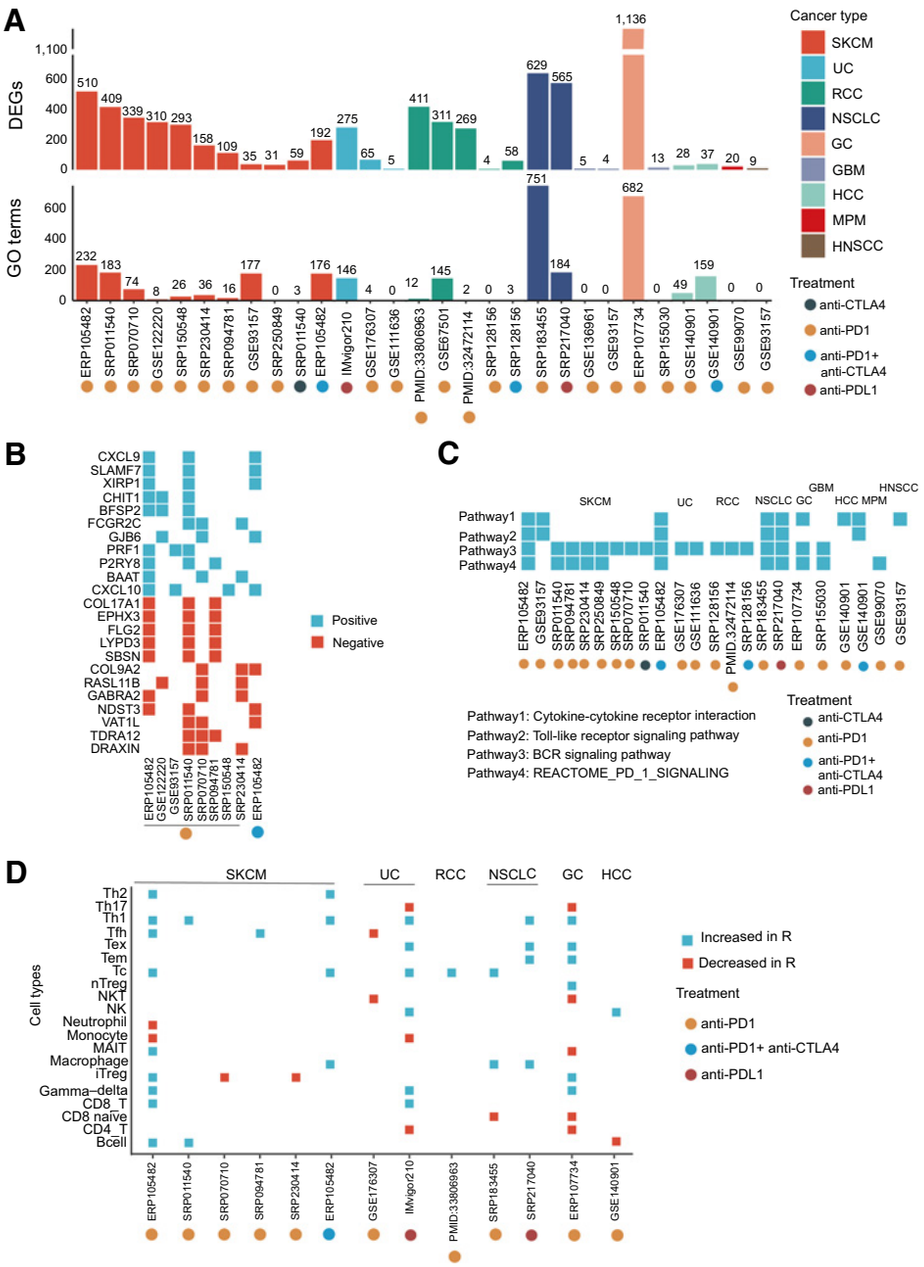

Figure 2.

Transcriptomic difference between R and NR based on pretreatment patients. **A,** Bar chart showing the numbers of DEGs (above), and GO terms enriched by them (bottom) with significant statistical difference. Color of the bar indicates different cancer types. Circles filled by different color in the bottom represent for different treatments. Level of statistical significance: DEGs ($|\log_2 FC|>1$ and FDR <0.05 or $|\log_2 FC|>1$ and P <0.05); GO terms (P_{adjust} < 0.05). **B,** Heat map showing the presence of some significant DEGs shared by samples from patients with anti–PD-1–treated melanoma. Positive, upregulated in responders. Negative, downregulated in responders. **C,** Heat map showing shared pathways among multiple data sets enriched by positive genes. **D,** Immune cells with significantly different distribution between responders and nonresponders (unpaired two-sided Wilcoxon test P < 0.05). Blue represents cell types with higher infiltration in responders, and red represents a higher infiltration in nonresponders.

immune cell types in samples. The result demonstrated that the Tc, Tex, Th1 cells, and macrophages were significantly higher in the responders across multiple data sets or cancer types (**Fig. 2D**). Moreover, hundreds of risk and protective genes were identified by the survival analysis. High CXCL9, and CXCL10 expression were significantly associated with a better prognosis for overall survival (OS) or progression-free survival (PFS) at least in two data sets or cancer types, which were also identified as upregulated genes in the responders (Supplementary Fig. S1A and S1B). The comparison results for Pre and On showed that the expression of some genes (e.g., CXCL9, PDCD1, and LAG3) were significantly increased in more than one data set after the ICB treatment (Supplementary Fig. S2A and S2B). Some signaling pathways, including the cytokine–cytokine receptor interaction, PD-1 signaling, and BCR signaling pathway, were also significantly enriched by the upregulated genes in the on-treatment samples. The immune cell distribution analysis result indicated that the abundance of the gamma–delta T and Th1 cells was significantly elevated after treatment, whereas neutrophils exhibited the opposite (Supplementary Fig. S2C).

Identifying response signatures in ICBatlas

We introduced the RS calculated on the basis of the fold-change and the universality of the DEGs at the data set or cancer type level to make it more intuitive for users to learn the degree of gene impact on the ICB response (see Materials and Methods section for details).The degree of gene impact on the ICB response was positively associated with the absolute value of the RS (i.e., genes with a positive RS were upregulated in responders and contributed

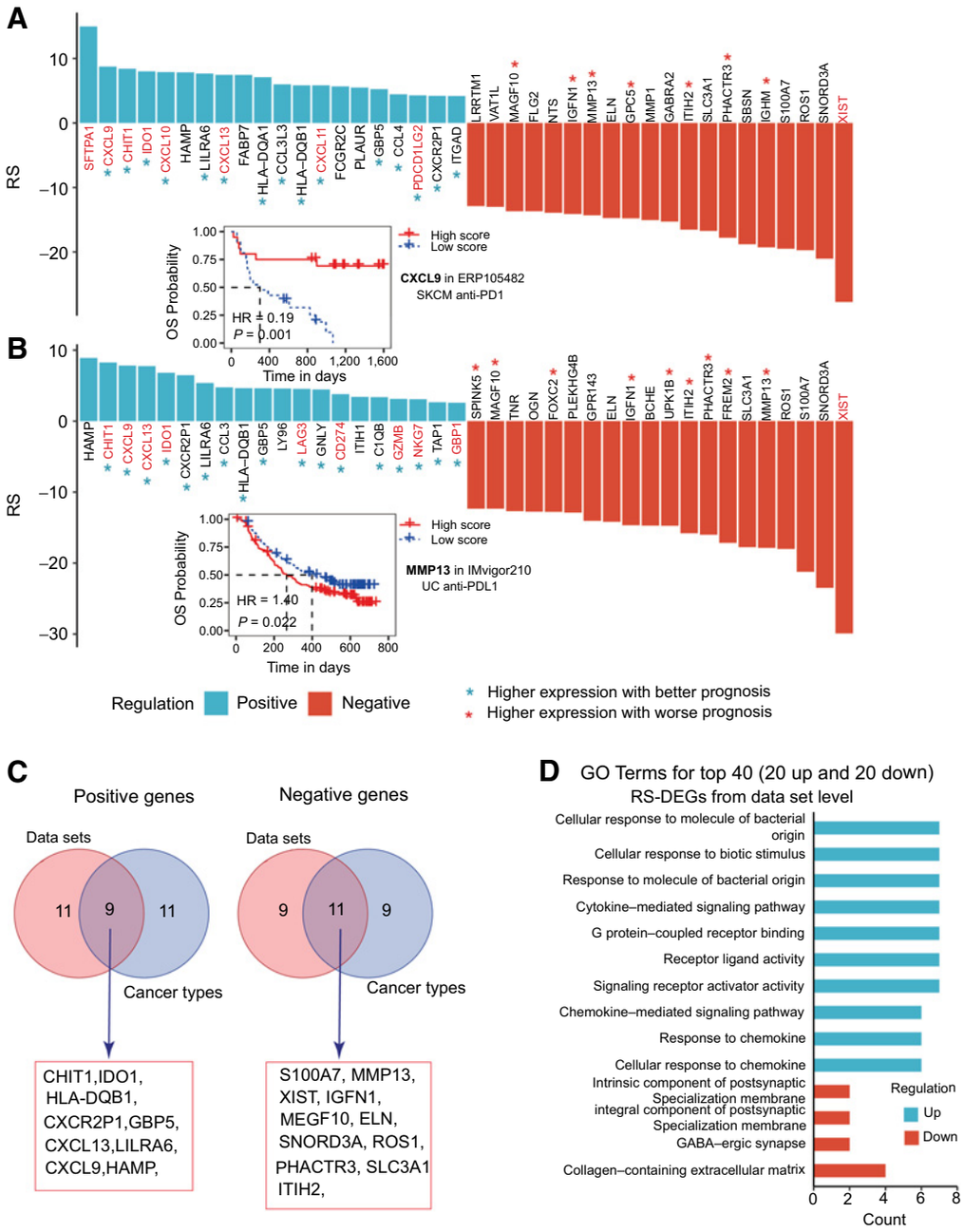

Figure 3.

Summary of top genes and pathways ranked by response score (RS) from data set and cancer type levels. **A** and **B,** Bar plots showing top 40 genes ranked by RS (20 positive and 20 negative) from data set level (**A**) and cancer type level (**B**). Genes with a blue bar were positive genes, which expressed higher in responders. Oppositely, genes with red bar were negative genes, which expressed higher in nonresponders. Genes in red-font are those have been reported to be related with the ICB therapy (response or nonresponse) in the literature. Kaplan–Meier plots showing prognosis by expression of CXCL9 or MMP13 in select data sets. OS, overall survival. HR, hazard ratio. A *P* value was calculated by Cox regression. **C,** Venn diagram showing the overlap of top 40 genes ranked by the positive (left) and negative (right) RS from data set and cancer-type levels. **D,** GO terms enriched from the top 40 genes (20 positive and 20 negative) from the data set level. Count represents the number of genes in the enriched terms.

to good prognosis, whereas genes with a negative RS exhibited the opposite). We systematically analyzed the top 20 genes ranked by the positive and negative RS (**Fig. 3A** and **B**). Note that some genes were shared between the data set and cancer type levels (e.g., IDO1, CXCL9/13, and CHIT1 with a positive RS and XIST with a negative RS; **Fig. 3C**), which may have more potential to serve as biomarkers in ICB therapy. There are also genes whose RS is particularly associated with specific cancer types. For example, the RS of TYRP1

is specifically high in SKCM (RS = −18.18), which is reported to be associated with response to anti–PD-1 therapy and can serve as a prognostic factor in melanoma. We also conducted literature research on the abovementioned genes, with the result, indicating that seven of 20 genes with a positive RS serve a good prognosis in ICB therapy (e.g., increased CXCL9/10, and IDO1; refs. 38–43). The high CXCL9/10 expression was particularly indicative of a good prognosis in SKCM (OS and PFS) and UC (OS; Supplementary Fig. S1). For genes with a negative RS, only XIST was reported to present a poor prognosis (42). In other words, genes identified by previous research to associate with positive prognosis are more likely to be identified in our model of gene expression associations. The study of genes contributing to a poor prognosis is also important, and our database may provide meaningful clues in this regard.

To further investigate the biological function of response-related genes, we selected the top 20 genes ranked by the positive and negative RS to conduct a pathway enrichment analysis. The result shows that genes with a positive RS were mainly enriched in the immune- and cellular response–related pathways, such as cellular response to biotic stimulus, signaling receptor activator activity, response to chemokine, chemokine-mediated signaling pathway, and cellular response to molecule of bacterial origin (**Fig. 3D**). In contrast, genes with a negative RS were mainly enriched in cell damage–related pathways, such as the cell junction assembly and the external encapsulating structure organization.

User-friendly interactive web interface for ICBatlas

All the abovementioned data and results were ultimately integrated into the ICBatlas database. The website consists of four main functional components: "Response (R vs. NR)," "Treatment (Pre vs. On)," "RS," and "Search" (**Fig. 4**). The contents in the "Response (R vs. NR)" and "Treatment (Pre vs. On)" modules were included at the data set, cancer, and immune checkpoint levels (**Fig. 4A** and **B**) to provide comprehensive information on ICB therapy to users. The items displayed at each level include the significant DEGs, GO and KEGG pathway terms, GSEA and GSVA gene sets, immune cells, and survival risk between the samples in different groups (i.e., R vs. NR and Pre vs. On). The RS module provides a scoring system (RS) for evaluating the degree of gene impact on the ICB response at the data set or cancer level (**Fig. 4C**), through which users can evaluate which genes have a greater potential to serve as an ICB response biomarker. In the "Search" module, ICBatlas provides multiple ways users can enter queries. First, a quick search box is located on the top panel of each page for querying by one specified gene symbol. Second, a universal search function for genes, pathways (gene sets), and immune cells (**Fig. 4D**) is provided, making it convenient for users to retrieve interesting information related to ICB therapy.

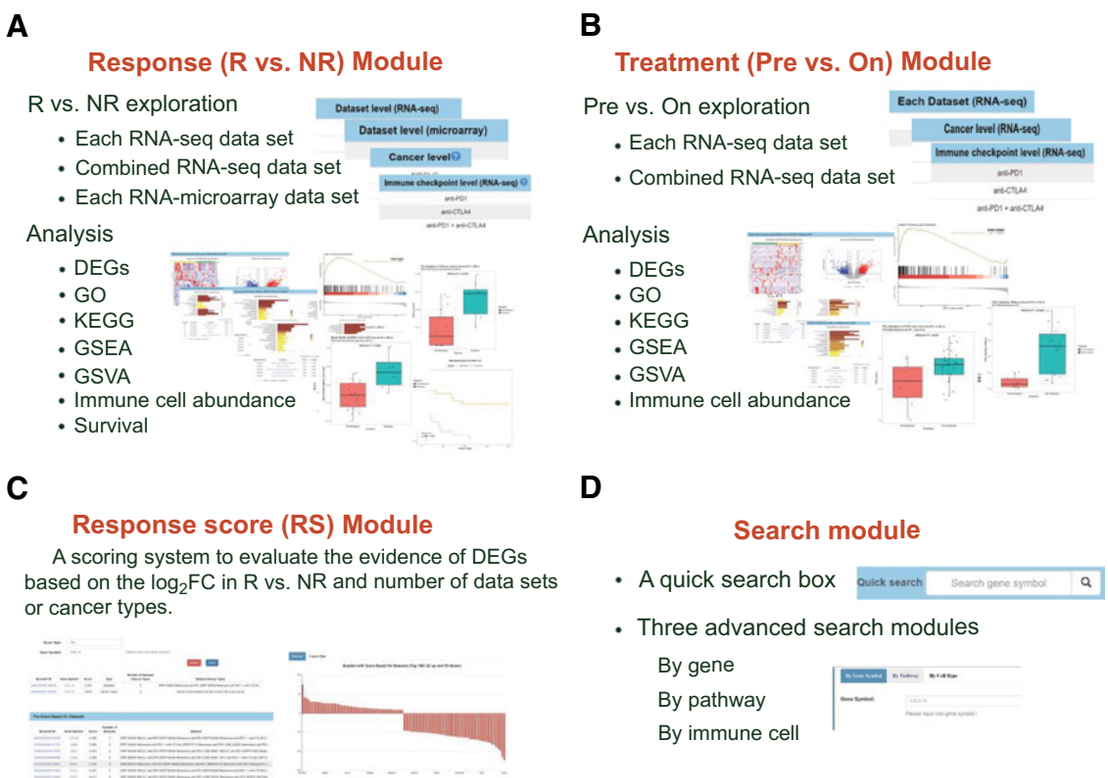

Figure 4.

Overview of the ICBatlas web-based resource. **A** and **B,** Response and treatment pages. The available tables and related plots (enrichment plot, box plot, and survival) are listed. **C,** The Response Score (RS) page provides a scoring system. For each positive gene, a higher absolute score indicates that the gene is relevant to ICB response with a higher confidence. **D,** Search modules in ICBatlas, including quick search and advanced search.

Discussion

ICBatlas is the first comprehensive expression resource for analyzing, curating, and visualizing the transcriptomic characteristics of ICB therapy based on human patient data. The database is composed of content that covers comparisons of the R vs. NR and Pre vs. On groups at the data set, cancer and immune checkpoint levels, demonstrating unique advantages over other related resources. First, it has the most comprehensive human ICB data to date, ideal for academic research. Second, the database modules are especially informative for researchers to rapidly investigate the impact of candidate genes, pathways, or immune cells on ICB therapy from large-scale data. Third, ICBatlas will facilitate the process for validating hypotheses and developing potential biomarkers to predict response to ICB therapies, as well as reduce the potential for erroneous conclusions drawn from a single data set.

Although ICBatlas collected and reanalyzed nearly all publicly available transcriptome data sets from the samples with ICB therapy, the limited cancer type and the limited sample numbers in some data sets remained inadequate, which may lead to bias in the analysis result. In the future, we will continue to collect additional available data and implement more functional modules related to the ICB therapy response to update ICBatlas regularly. ICBatlas will serve as a comprehensive resource and data reuse tool for researchers of cancer immune-related topics and will provide novel insights into for ICB response and resistance.

Authors' Disclosures

No disclosures were reported.

Authors' Contributions

M. Yang: Resources, data curation, software, visualization, writing–original draft. **Y.-R. Miao:** Methodology, writing–review and editing. **G.-Y. Xie:** Software, methodology. **M. Luo:** Software. **H. Hu:** Software. **H.F. Kwok:** Writing–review and editing. **J. Feng:** Conceptualization, project administration. **A.-Y. Guo:** Project administration, writing–review and editing.

Acknowledgments

The ICBatlas was constructed on the basis of integrating public ICB therapy RNA-seq and microarray data sets. We acknowledge all the researchers and participants to share their data sets. All the contributors are listed on our website. This work was supported by National Key R&D Program of China (2021YFF0703704); Natural Science Foundation for Distinguished Young Scholars of Hubei Province of China (2020CFA070); Science, Technology and Innovation Commission of Shenzhen Municipality (JCYJ20210324141814037).

The publication costs of this article were defrayed in part by the payment of publication fees. Therefore, and solely to indicate this fact, this article is hereby marked "advertisement" in accordance with 18 USC section 1734.

Note

Supplementary data for this article are available at Cancer Immunology Research Online (http://cancerimmunolres.aacrjournals.org/).

Received March 29, 2022; revised June 30, 2022; accepted September 8, 2022; published first September 12, 2022.

References

1. Hamid O, Robert C, Daud A, Hodi FS, Hwu W-J, Kefford R, et al. Safety and tumor responses with lambrolizumab (anti–PD-1) in melanoma. N Engl J Med 2013;369:134–44.
2. Topalian SL, Hodi FS, Brahmer JR, Gettinger SN, Smith DC, McDermott DF, et al. Safety, activity, and immune correlates of anti–PD-1 antibody in cancer. N Engl J Med 2012;366:2443–54.
3. Kim ST, Cristescu R, Bass AJ, Kim K-M, Odegaard JI, Kim K, et al. Comprehensive molecular characterization of clinical responses to PD-1 inhibition in metastatic gastric cancer. Nat Med 2018;24:1449–58.
4. Powles T, Eder JP, Fine GD, Braiteh FS, Loriot Y, Cruz C, et al. MPDL3280A (anti–PD-L1) treatment leads to clinical activity in metastatic bladder cancer. Nature 2014;515:558–62.
5. Kang Y-K, Boku N, Satoh T, Ryu M-H, Chao Y, Kato K, et al. Nivolumab in patients with advanced gastric or gastro-oesophageal junction cancer refractory to, or intolerant of, at least two previous chemotherapy regimens (ONO-4538–12, ATTRACTION-2): a randomised, double-blind, placebo-controlled, phase 3 trial. Lancet 2017;390:2461–71.
6. Muro K, Chung HC, Shankaran V, Geva R, Catenacci D, Gupta S, et al. Pembrolizumab for patients with PD-L1–positive advanced gastric cancer (KEYNOTE-012): a multicentre, open-label, phase 1b trial. Lancet Oncol 2016;17:717–26.
7. Topalian SL, Sznol M, McDermott DF, Kluger HM, Carvajal RD, Sharfman WH, et al. Survival, durable tumor remission, and long-term safety in patients with advanced melanoma receiving nivolumab. J Clin Oncol 2014;32:1020–30.
8. Ribas A, Wolchok JD. Cancer immunotherapy using checkpoint blockade. Science 2018;359:1350–5.
9. Gide TN, Quek C, Menzies AM, Tasker AT, Shang P, Holst J, et al. Distinct immune cell populations define response to anti–PD-1 Monotherapy and anti–PD-1/anti–CTLA-4 combined therapy. Cancer Cell 2019;35:238–55.e6.
10. Riaz N, Havel JJ, Makarov V, Desrichard A, Urba WJ, Sims JS, et al. Tumor and microenvironment evolution during immunotherapy with nivolumab. Cell 2017;171:934–49.
11. Jiang P, Gu S, Pan D, Fu J, Sahu A, Hu X, et al. Signatures of T-cell dysfunction and exclusion predict cancer immunotherapy response. Nat Med 2018;24:1550–8.
12. Somasundaram R, Connelly T, Choi R, Choi H, Samarkina A, Li L, et al. Tumor-infiltrating mast cells are associated with resistance to anti–PD-1 therapy. Nat Commun 2021;12:346.
13. Shahabi V, Berman D, Chasalow SD, Wang L, Tsuchihashi Z, Hu B, et al. Gene expression profiling of whole blood in ipilimumab-treated patients for identification of potential biomarkers of immune-related gastrointestinal adverse events. J Transl Med 2013;11:75.
14. Lozano AX, Chaudhuri AA, Nene A, Bacchiocchi A, Earland N, Vesely MD, et al. T-cell characteristics associated with toxicity to immune checkpoint blockade in patients with melanoma. Nat Med 2022;28:353–62.
15. Jing Y, Liu J, Ye Y, Pan L, Deng H, Wang Y, et al. Multi-omics prediction of immune-related adverse events during checkpoint immunotherapy. Nat Commun 2020;11:4946.
16. Rooney MS, Shukla SA, Wu CJ, Getz G, Hacohen N. Molecular and genetic properties of tumors associated with local immune cytolytic activity. Cell 2015;160:48–61.
17. Ayers M, Lunceford J, Nebozhyn M, Murphy E, Loboda A, Kaufman DR, et al. IFN-γ–related mRNA profile predicts clinical response to PD-1 blockade. J Clin Invest 2017;127:2930–40.
18. Auslander N, Zhang G, Lee JS, Frederick DT, Miao B, Moll T, et al. Robust prediction of response to immune checkpoint blockade therapy in metastatic melanoma. Nat Med 2018;24:1545–9.
19. Hu F-F, Liu C-J, Liu L-L, Zhang Q, Guo A-Y. Expression profile of immune checkpoint genes and their roles in predicting immunotherapy response. Brief Bioinform 2021;22:bbaa176.
20. Hugo W, Zaretsky JM, Sun L, Song C, Moreno BH, Hu-Lieskovan S, et al. Genomic and transcriptomic features of response to anti–PD-1 therapy in metastatic melanoma. Cell 2016;165:35–44.
21. Zhang Y, Yao Y, Chen P, Liu Y, Zhang H, Liu H, et al. Checkpoint therapeutic target database (CKTTD): the first comprehensive database for checkpoint

targets and their modulators in cancer immunotherapy. J Immunother Cancer 2020;8:e001247.
22. Sun D, Wang J, Han Y, Dong X, Ge J, Zheng R, et al. TISCH: a comprehensive web resource enabling interactive single-cell transcriptome visualization of tumor microenvironment. Nucleic Acids Res 2021; 49:D1420–30.
23. Zeng Z, Wong CJ, Yang L, Ouardaoui N, Li D, Zhang W, et al. TISMO: syngeneic mouse tumor database to model tumor immunity and immunotherapy response. Nucleic Acids Res 2021;gkab804.
24. Eisenhauer EA, Therasse P, Bogaerts J, Schwartz LH, Sargent D, Ford R, et al. New response evaluation criteria in solid tumours: revised RECIST guideline (version 1.1). Eur J Cancer 2009;45:228–47.
25. Kim D, Paggi JM, Park C, Bennett C, Salzberg SL. Graph-based genome alignment and genotyping with HISAT2 and HISAT-genotype. Nat Biotechnol 2019;37: 907–15.
26. Li H, Handsaker B, Wysoker A, Fennell T, Ruan J, Homer N, et al. The sequence alignment/map format and SAMtools. Bioinformatics 2009;25:2078–9.
27. Liao Y, Smyth GK, Shi W. featureCounts: an efficient general purpose program for assigning sequence reads to genomic features. Bioinformatics 2014;30:923–30.
28. Zhang Y, Parmigiani G, Johnson WE. ComBat-seq: batch effect adjustment for RNA-seq count data. NAR Genom Bioinform 2020;2:lqaa078.
29. Love MI, Huber W, Anders S. Moderated estimation of fold change and dispersion for RNA-seq data with DESeq2. Genome Biol 2014;15:550.
30. Ritchie ME, Phipson B, Wu D, Hu Y, Law CW, Shi W, et al. limma powers differential expression analyses for RNA-sequencing and microarray studies. Nucleic Acids Res 2015;43:e47.
31. Wu T, Hu E, Xu S, Chen M, Guo P, Dai Z, et al. clusterProfiler 4.0: a universal enrichment tool for interpreting omics data. Innovation 2021;2: 100141.
32. Subramanian A, Tamayo P, Mootha VK, Mukherjee S, Ebert BL, Gillette MA, et al. Gene set enrichment analysis: a knowledge-based approach for interpreting genome-wide expression profiles. Proc Natl Acad Sci U S A 2005;102:15545–50.
33. Hänzelmann S, Castelo R, Guinney J. GSVA: gene set variation analysis for microarray and RNA-seq data. BMC Bioinf 2013;14:7.
34. Bhattacharya S, Andorf S, Gomes L, Dunn P, Schaefer H, Pontius J, et al. ImmPort: disseminating data to the public for the future of immunology. Immunol Res 2014;58:234–9.
35. Charoentong P, Finotello F, Angelova M, Mayer C, Efremova M, Rieder D, et al. Pan-cancer immunogenomic analyses reveal Genotype-immunophenotype relationships and predictors of response to checkpoint blockade. Cell Rep 2017;18:248–62.
36. Miao Y-R, Zhang Q, Lei Q, Luo M, Xie G-Y, Wang H, et al. ImmuCellAI: a unique method for comprehensive T-cell subsets abundance prediction and its application in cancer immunotherapy. Adv Sci 2020;7:1902880.
37. Li T, Fu J, Zeng Z, Cohen D, Li J, Chen Q, et al. TIMER2.0 for analysis of tumor-infiltrating immune cells. Nucleic Acids Res 2020;48:W509–14.
38. House IG, Savas P, Lai J, Chen AXY, Oliver AJ, Teo ZL, et al. Macrophage-derived CXCL9 and CXCL10 are required for antitumor immune responses following immune checkpoint blockade. Clin Cancer Res 2020; 26:487–504.
39. Bassez A, Vos H, Van Dyck L, Floris G, Arijs I, Desmedt C, et al. A single-cell map of intratumoral changes during anti-PD1 treatment of patients with breast cancer. Nat Med 2021;27:820–32.
40. Litchfield K, Reading JL, Puttick C, Thakkar K, Abbosh C, Bentham R, et al. Meta-analysis of tumor- and T-cell–intrinsic mechanisms of sensitization to checkpoint inhibition. Cell 2021;184:596–614.e14.
41. Jiang Y-Q, Wang Z-X, Zhong M, Shen L-J, Han X, Zou X, et al. Investigating mechanisms of response or resistance to immune checkpoint inhibitors by analyzing cell–cell communications in tumors before and after programmed cell death-1 (PD-1) targeted therapy: an integrative analysis using single-cell RNA and bulk-RNA sequencing data. OncoImmunology 2021;10:1908010.
42. Zhang Y, Yang Q, Zeng X, Wang M, Dong S, Yang B, et al. MET amplification attenuates lung tumor response to immunotherapy by inhibiting STING. Cancer Discov 2021;11:2726–37.
43. Zhao R, Li B, Zhang S, He Z, Pan Z, Guo Q, et al. The N6-methyladenosine-modified pseudogene HSPA7 correlates with the tumor microenvironment and predicts the response to immune checkpoint therapy in glioblastoma. Front Immunol 2021;12:653711.